PERGAMON

International Journal of Heat and Mass Transfer 45 (2002) 793–801

International Journal of HEAT and MASS TRANSFER

www.elsevier.com/locate/ijhmt

Influence of the Prandtl number on the location of recirculation eddies in thermocapillary flows

Jean-François Mercier [1], Christiane Normand *

CEA/Saclay, Service de Physique Théorique, F-91191 Gif-sur-Yvette Cedex, France

Received 10 March 2001; received in revised form 29 May 2001

Abstract

Two-dimensional thermocapillary-driven flow in a horizontal cavity of large aspect ratio is considered. Of particular interest is the asymptotic matching between the known parallel core flow solution and the non-parallel flow near the ends of the cavity. The influence of the end regions on the core flow is described by the superposition of spatial disturbances to the core flow solution. The stability analysis of this perturbed state leads to an eigenvalue problem for the complex wave number of the disturbances. The end flow structures are related to the nature of the lowest eigenvalue: when purely real it describes a boundary layer regime whereas a non-vanishing imaginary part reveals the existence of periodic structures known as recirculation rolls or eddies. It is found that, depending on the Prandtl number value, Pr, recirculation eddies can exist either near the hot wall ($Pr \gg 1$) or the cold wall ($Pr \ll 1$). Our results provide a direct interpretation to the different behaviors observed in previous experimental and numerical studies.

Keywords: Thermocapillary flows; Recirculation eddies

1. Introduction

Thermocapillary driven flows have received an increasing attention during the past several years, especially because of their importance in material processing technologies, such as semiconductors crystal growth from the melt. The dynamics observed in applications are very complex and fundamental studies have dealt with a simplified geometry where the underlying physical mechanisms are easier to track.

We are presently interested in flows developing in a rectangular cavity filled with a fluid whose top surface open to ambient air has surface tension acting on it. A horizontal temperature gradient is applied, by differentially heating two of the opposite vertical walls confining the fluid laterally. Experiments conducted in this configuration differ by the extent of the heated sidewalls, being either longer [1,2], or shorter [3,4], than the width between them. Whatever the length of the heated walls is, the primary flow is considered as mostly two-dimensional and sensitivity to the geometry only manifests when instability occurs in the system. Transverse disturbances are preferentially observed when the differentially heated walls have a short extent while longitudinal or oblique disturbances are only seen in the opposite situation. In a rectangular cavity with equal length and width, Braunsfurth and Homsy [5] have observed a novel oscillatory flow arising as a secondary instability after the primary steady longitudinal rolls.

Most of the theoretical studies on thermocapillary-driven flows have been concerned with the temporal stability analysis of plane-parallel flows in an infinite horizontal layer [6–10]. However, the approximation of a plane-parallel flow is only valid in the core region far from the vertical walls confining the fluid laterally. Indeed, numerical and experimental studies revealed that the side walls can strongly distort the plane-parallel thermocapillary flow, even below the threshold for onset of

* Corresponding author. Tel.: +33-1-69-08-80-08; fax: +33-1-69-08-81-20.

E-mail address: normand@spht.saclay.cea.fr (C. Normand).

[1] Present address: Laboratoire de Simulation et de Modélisation des phénomènes de Propagation, URA 853-CNRS, ENSTA, 32 Bld Victor, Paris 75739 Cedex 15, France.

0017-9310/02/$ - see front matter
PII: S0017-9310(01)00185-5

Nomenclature

a	real part of the complex wave number α
A	aspect ratio, $A = L/h$
b	imaginary part of the complex wave number α
D	derivative with respect to the vertical coordinate z
g	gravity acceleration
h	height of fluid
l	penetration length
L	horizontal extent of the fluid layer
Ma	Marangoni number, $Ma = RePr$
p	pressure
Pr	Prandtl number, $Pr = \nu/\kappa$
Re	Reynolds number, $Re = U_s h/\nu$
t	time
T	fluid temperature
T_0	temperature of the cold vertical wall
T_1	temperature of the hot vertical wall
u	horizontal component of the velocity
u_0	horizontal velocity of the base flow
U_s	characteristic velocity
w	vertical component of the velocity
x	horizontal coordinate
x_0	position of the end wall
z	vertical coordinate

Greek symbols

α	complex wave number
β_T	horizontal temperature gradient
γ	derivative of surface tension with respect to temperature
η	dynamical viscosity
θ_1	temperature perturbation
$\theta(z)$	vertical dependence of the temperature perturbation
κ	thermal diffusivity
ν	kinematic viscosity
ρ	fluid density
σ	surface tension
σ_0	reference surface tension
$\tau_0(z)$	vertical temperature distribution associated to the base flow
$\phi(z)$	vertical dependence of the stream function perturbation
ψ	stream function
ψ_1	stream function perturbation

hydrothermal waves predicted to be the most dangerous modes of instability in an unbounded fluid layer.

Numerical simulations of thermocapillary convection developing in rectangular cavities of large horizontal extent have essentially dealt with two-dimensional flows, three-dimensional effects being only considered in a cubic cavity [11]. In the case of low Prandtl number fluids, Ben Hadid and Roux [12] performed calculations in a rectangular cavity bounded by two horizontal surfaces, either both conducting or both insulating. For low values of the Marangoni number, the fluid circulation in the whole layer is monocellular and symmetric with respect to the vertical midplane. When the Marangoni number is increased, the apparition of recirculation rolls is reported near the cold wall whereas near the hot wall the viscous flow gives way to a boundary layer regime. The number of recirculation rolls depends on the Marangoni number value and on the aspect ratio of the fluid layer. When thermocapillarity is the only driving mechanism, Ben Hadid and Roux calculations always converged to a steady flow and buoyancy effects needed to be included [13] to capture temporal oscillations in the fluid. Considering a fluid with a higher Prandtl number $Pr = 4$, Villers and Platten [14] obtained a result opposite to Ben Hadid and Roux finding, with the apparition of recirculation rolls near the hot wall and a boundary layer regime near the cold wall, like Mundrane and Zebib [15] when investigating a fluid of still larger Prandtl number $Pr = 8.4$. These different behaviors of the fluid near the vertical walls when the Prandtl number varies were also reported by Zebib et al. [16], for fluids of Prandtl numbers ranging between $Pr = 0.05$ and 50, confirming that recirculation rolls develop near the cold wall for low Prandtl numbers and near the hot wall for high Prandtl numbers.

Some of these numerical results have been validated by experimental observations. To illustrate the best our purpose we shall focus on those studies carried out in rectangular cavities with a large extent in the streamwise direction and a narrow one in the spanwise direction, so as to prevent from the onset of three-dimensional instability. To allow for visualization of the flow structure, most of these experiments have been conducted in transparent fluids which have moderate or large Prandtl numbers. Thus, beside the numerical study mentioned above, Villers et Platten [14] also conducted experiments using acetone, a fluid of Prandtl number ($Pr = 4$) and observed the apparition of recirculation rolls near the hot wall. With still higher Prandtl number fluids, respectively, $Pr = 15$ and 17, De Saedleer et al. [3] and Schwabe et al. [17] also observed the development of several rolls near the hot wall. Moreover, De Saedleer et al. measured the vertical velocity on the whole length of the cavity and showed that the amplitude of the velocity is exponentially decaying with distance from the hot wall. In a larger range of Prandtl number

($Pr = 10$–30), Garcimartin et al. [4] still found the apparition of an intense roll near the hot side of the cavity, followed by several less intense rolls. When increasing the imposed temperature gradient, these authors observed that the rolls begin to oscillate and then propagate from the hot side to the cold side. The important point to notice is that this phenomenon cannot be assimilated to the hydrothermal waves predicted by Smith et Davis [6] in an unbounded fluid layer, which propagate from the cold region to the hot region. Thus, the dynamics generated by the lateral walls possibly affect the instability patterns predicted for an unbounded layer.

In most of the references cited above the lateral boundaries were straight walls but a few of them dealt with cylindrical walls [17]. This is also the case in [18,19] where Favre et al. studied two fluids with very different Prandtl numbers, respectively, silicon oil and mercury. In their experimental device, the fluid filling a cylindrical vessel is locally heated on the top free surface and the base flow takes the form of a torus. For silicon oil, $Pr = 10$, recirculation rolls appear near the cylindrical heater as it is also confirmed by numerical simulations. For mercury, $Pr = 0.02$, visualization cannot be implemented and the knowledge of end circulation comes from numerical results showing the presence of recirculation eddies near the cooled outer cylindrical wall. This confirms that the change in the flow structure near the side walls according to the value of the Prandtl number is independent of the geometry.

An alternative approach to numerical simulations was proposed by Laure et al. [20] who addressed the problem of the end wall circulations in thermocapillary flows in the case of a zero Prandtl number fluid. They considered that sidewalls induce perturbations to the parallel core flow, which can be decomposed into spatial modes with complex wave numbers. The stability analysis provides the less attenuated modes and revealed the presence of recirculation rolls near the cold vertical wall. Their analysis was reminiscent of the asymptotic matching procedure used by Daniels [21] when considering the problem of end circulation for a buoyant flow in a vertical slot with differentially heated walls. This is a powerful approach to get insight into the flow structure near the end walls which is not restricted to thermally driven flows and has been used in various other hydrodynamic systems. In a pioneering work, Bye [22] described the end circulations of a Couette–Poiseuille flow in a rectangular cavity, due to a constant stress (surface wind) acting on the free surface of the fluid layer. By analyzing the stability of the base flow with respect to spatial disturbances associated to a complex wave number, Bye concluded that recirculation rolls appear downwind while a boundary layer regime takes place upwind. An experimental investigation by Neary and Stephanoff [23] of the shear-driven flow in an open cavity confirms that a recirculation roll develops in the downstream-third of the cavity.

Considering flows with curved streamlines, Normand et al. [24] demonstrated the existence of recirculation eddies in the Taylor–Dean flow between two horizontal coaxial cylinders with a partially filled gap. They found that when the two cylinders are counter-rotating, recirculation rolls develop on both free end surfaces whereas the rolls appear only near one of the free surfaces when the cylinders are co-rotating.

The present contribution [25] is an extension of Laure et al. analysis [20] to establish the influence of the Prandtl number value on the location of the recirculation eddies that have been observed either near the hot or the cold sidewalls in thermocapillary-driven flows. We shall focus on the distortions to the steady parallel core flows before the onset of temporal modes of instability and do not intend to describe the influence of the lateral walls on the instability pattern.

2. Spatial modes analysis

We consider an incompressible fluid filling a rectangular cavity of height h and of length $L \gg h$, bounded below by a rigid surface and above by a free surface (see Fig. 1, where the core flow velocity is also represented). The top and bottom boundaries are considered insulating, as it is the case in most experimental studies and numerical simulations.

Introducing Cartesian coordinates, Ox will denote the horizontal axis, and Oz the vertical upward axis. The fluid layer is bounded laterally by two isothermal vertical walls maintained at different temperatures, respectively, $T = T_0$ at $x = 0$ and $T = T_1 > T_0$ at $x = L$. The horizontal temperature gradient $\beta_T = (T_1 - T_0)/L$ would produce a temperature distribution $T - T_0 = \beta_T x$ in a fluid at rest.

We consider a thin fluid layer where thermocapillary forces dominate buoyancy forces. Thus, the density ρ of the fluid is taken constant while linear variations of the surface tension σ with the fluid temperature T are considered according to the law

$$\sigma = \sigma_0 - \gamma(T - T_0),$$

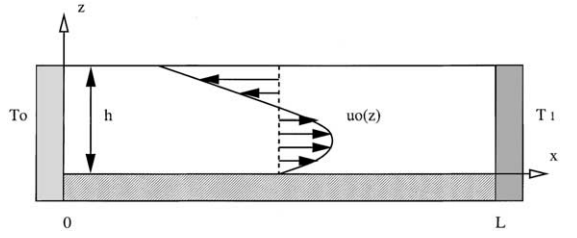

Fig. 1. Geometry of the fluid layer and core flow velocity $u_0(z)$.

where $\gamma = -\mathrm{d}\sigma/\mathrm{d}T$ is positive, as it is the case for most ordinary fluids, and $\sigma_0 = \sigma(T_0)$. The thermocapillary forces induced by the applied temperature gradient drive the fluid on the free surface from the hot areas toward the cold areas, resulting in a fluid circulation into the whole layer.

The velocity $\vec{u} = (u, w)$ and temperature T in the fluid satisfy the conservation equations for mass, momentum and energy which read

$$\vec{\nabla} \cdot \vec{u} = 0, \tag{1}$$

$$\left(\frac{\partial}{\partial t} + \vec{u} \cdot \vec{\nabla}\right)\vec{u} = -\frac{1}{\rho}\vec{\nabla}p + \vec{g} + \nu\Delta\vec{u}, \tag{2}$$

$$\left(\frac{\partial}{\partial t} + \vec{u} \cdot \vec{\nabla}\right)T = \kappa\Delta T, \tag{3}$$

where p is the fluid pressure, ν the kinematic viscosity and κ the thermal diffusivity. We shall distinguish two regions in the fluid, the core region where the velocity has only one component $u = U_0(z)$ in the x-direction and two end regions where the vertical component of the velocity w can no longer be neglected.

In the core region, the momentum equation (2) simplifies in $D^3U_0 = 0$, where $D \equiv \mathrm{d}/\mathrm{d}z$ denotes the derivative with respect to the vertical coordinate. On the free surface at $z = h$, the balance between the viscous tangential stress and the thermocapillary force expresses as

$$\eta DU_0 = -\gamma\beta_T.$$

Taking h as the typical length scale, this relation provides the typical velocity scale $U_s = \gamma\beta_T h/\eta$ so that the base flow velocity is written $U_0 = U_s u_0$. Using the boundary condition on the rigid bottom plate $u_0 = 0$, and the flux conservation through any vertical plane $\int_0^1 u_0\,\mathrm{d}z = 0$, the base flow velocity reads in a non-dimensional form

$$u_0(z) = -\frac{z(3z-2)}{4}.$$

In Eq. (3), the convective heat transport $(\vec{u} \cdot \vec{\nabla})T \propto \beta_T u_0$ should be balanced by a vertical temperature distribution $\tau_0(z)$ that adds to the horizontal temperature distribution. Taking $\beta_T h$ as the typical scale for the temperature, then $T - T_0 = x + Ma\,\tau_0(z)$, where $Ma = U_s h/\kappa$ is the Marangoni number. Eq. (3) becomes $u_0 = D^2\tau_0$, to be solved with the boundary conditions $D\tau_0 = 0$, on $z = 0$ and $z = 1$, leading to the vertical temperature gradient

$$D\tau_0 = -\frac{z^2(z-1)}{4}.$$

The plane-parallel flow approximation is only valid in the core of the fluid layer far from the isothermal vertical walls confining the fluid laterally where the flow is distorted and becomes two-dimensional. Therefore, we can introduce the stream function $\psi(x, z)$ such that

$$u = \frac{\partial\psi}{\partial z} \quad \text{and} \quad w = -\frac{\partial\psi}{\partial x}.$$

The deformations of the core flow due to the vertical walls at $x = 0$ and $x = A$ where $A = L/h$ is the aspect ratio of the cavity, are analyzed by considering that the lateral walls induce a perturbation in the fluid, characterized by a stream function ψ_1 and a temperature θ_1 decaying spatially when approaching the parallel core flow solution. The perturbations are sought in the form

$$\psi_1 = \phi(z)\exp[\alpha(x - x_0)],$$
$$\theta_1 = \theta(z)\exp[\alpha(x - x_0)].$$

According to the location of the wall we are studying the influence on the base flow, x_0 will take two different values: when looking for the behavior of the fluid close to the cold side wall we shall consider $x_0 = 0$ with $x > 0$ and $\psi_1 \to 0$ when $x \to \infty$. Whereas close to the hot side wall we shall consider $x_0 = A$ with $x - x_0 < 0$ and $\psi_1 \to 0$ when $x - x_0 \to -\infty$.

The wave number $\alpha = a + \mathrm{i}b$ is a complex quantity. Its real part a is related to the spatial attenuation rate of the perturbations when going away from the vertical walls, and is equal to the inverse of the penetration length l of the perturbations $|a| = 1/l$. The exponential spatial decay of the perturbations was detected in experiments by De Saedleer et al. [3] through measurements of the vertical velocity near the hot wall. The imaginary part b is related to the wavelength of the perturbation $\lambda = 2\pi/b$. Moreover, the sign of the real part of α indicates the location of the perturbation: since the disturbances due to the vertical walls must decrease when approaching the core of the cavity, eigenvalues α with positive real parts are related to the behavior of the fluid in the vicinity of the hot wall located at $x = A$, whereas eigenvalues of negative real parts indicate the behavior of the flow close to the cold wall at $x = 0$.

The vertical dependence of the perturbations, $\phi(z)$ and $\theta(z)$, are solutions of the system obtained after linearization of Eqs. (2) and (3) around the core flow solution

$$(D^2 + \alpha^2)^2\phi = \alpha Re[u_0(D^2 + \alpha^2) - u_0'']\phi, \tag{4}$$

$$(D^2 + \alpha^2)\theta = Ma[\alpha(u_0\theta - Ma\tau_0'\phi) + D\phi], \tag{5}$$

where $Re = U_s h/\nu$ is the Reynolds number, $Ma = Re\,Pr$ is the Marangoni number and $Pr = \nu/\kappa$ is the Prandtl number. The associated boundary conditions are, for the stream function:

$$\begin{aligned} &\phi = 0,\ D\phi = 0 \quad \text{at } z = 0,\\ &\phi = 0,\ D^2\phi = -\alpha\theta \quad \text{at } z = 1, \end{aligned} \tag{6}$$

and for the temperature: $D\theta = 0$ on $z = 0$ and $z = 1$.

For a vanishing Reynolds number (and thus simultaneously the Marangoni number), the spectrum of eigenvalues α is found to be the same whatever is the value of the Prandtl number. The temperature, solution of

$$(D^2 + \alpha^2)\theta = 0, \tag{7}$$

leads to the eigenvalues $\alpha_n = n\pi$. The stream function, solution of the Stokes equation $(D^2 + \alpha^2)^2\phi = 0$, is coupled to the temperature through the boundary condition, $D^2\phi = -\alpha\theta$, thus satisfying an inhomogeneous differential system. The stream function is the sum of two contributions: one is a particular solution that shares a common eigenvalues spectrum with the temperature. The other contribution, independent of the temperature, satisfies the homogeneous boundary condition $D^2\phi = 0$ on $z = 1$ and it evolves according to its own eigenvalue spectrum with α_n solutions of

$$\sin(2\alpha) = 2\alpha. \tag{8}$$

We shall see in the next section how this two independent sets of eigenvalues evolve when the Reynolds number is increased. The results will be presented in different subsections according to the value of the Prandtl number.

2.1. Vanishing Prandtl number

Let us first consider the case of a fluid of high thermal conductivity compared to its viscosity ($Pr = 0$).

The evolution of the real part a of the eigenvalues α when the Reynolds number varies is represented in Fig. 2. Dashed lines denote real eigenvalues while solid lines denote complex eigenvalues. For $Re = 0$, the starting points are the "thermal" eigenvalues $\alpha_n = n\pi$, which have been drawn for the integer values, $n = \pm 1$ and 2, and the "hydrodynamic" eigenvalues solution of Eq. (8), whose two lowest values are

$$\alpha_1 = \pm 3.749 \pm i1.384,$$
$$\alpha_2 = \pm 6.950 \pm i1.676.$$

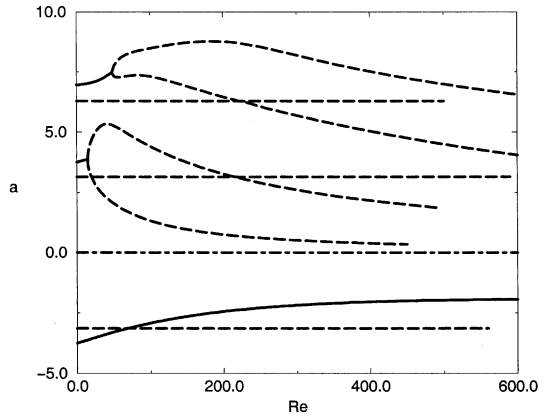

Fig. 2. Evolution of the real parts a of the eigenvalues α vs the Reynolds number Re, in the case $Pr = 0$. Solid lines: complex eigenvalues; dashed lines: real eigenvalues. The behavior near the hot (respectively, cold) wall is related to $a > 0$ (respectively, $a < 0$).

When the Reynolds number is increased, the thermal eigenvalues remain constant and equal to $\alpha_n = n\pi$ because the temperature equation (5), reduces to a purely conductive heat transfer equation (7) in the case $Ma = RePr = 0$. On the contrary the stream function equation (4) depends on Re and its spectrum evolves when the Reynolds number is increased. Each of the first two complex hydrodynamic eigenvalues with a positive real part splits into two real eigenvalues whereas the hydrodynamic eigenvalue with a negative real part remains complex. Since the real part of the eigenvalues is proportional to the inverse of the penetration length of the disturbances, the flow structure close to the vertical walls will be governed by the eigenvalues of smallest real parts. It is shown in Fig. 2 that the first hydrodynamic complex eigenvalue starting with a real part $a = 3.8$ for $Re = 0$, splits into two real eigenvalues for $Re = 15$, and then the lower eigenvalue remains real and tends towards zero. The hydrodynamic eigenvalue with a negative real part starting from $a = -3.8$ at $Re = 0$, remains complex and its real part slowly decreases when the Reynolds number is increased. The interpretation is that recirculation rolls appear in the vicinity of the cold wall ($a < 0,\ b \neq 0$) and penetrate further and further in the core of the fluid layer when the imposed temperature gradient is increased, whereas a boundary layer regime takes place close to the hot wall ($a > 0,\ b = 0$) replacing the viscous flow existing for $Re \to 0$, with a thickness layer $l = 1/a$. These results agree with numerical results obtained for fluids of small Prandtl number by Ben Hadid and Roux [12], Favre et al. [19], and Zebib et al. [16], who reported on the development of recirculation rolls near the cold vertical wall.

The case of a zero Prandtl number fluid was previously investigated by Laure et al. [20] when the two horizontal surfaces are conducting. Thus, the thermocapillary boundary condition $D^2\phi = -\alpha\theta$ at $z = 1$ reduces to $D^2\phi = 0$, and the two sets of eigenvalues, thermal and hydrodynamic, become independent. The temperature disturbances in the conducting case are $\theta(z) = \sin n\pi z$ instead of $\theta(z) = \cos n\pi z$ in the insulating case, the thermal eigenvalues being $\alpha_n = n\pi$ in both cases. This result also agrees with the assertion by Ben Hadid and Roux [12] that conducting or insulating boundary conditions lead to the same end structures when $Pr = 0$.

2.2. Infinite Prandtl number

Fluids of large viscosity compared to the thermal conductivity (fluid of infinite Prandtl number) have not received as much attention as the opposite situation ($Pr = 0$) at least from the numerical point of view, but there are many experimental results to compare with. We shall consider the Prandtl number going to infinity while the Marangoni number remains finite so that the Reynolds number tends towards zero.

In Fig. 3 are reported the variations of the real part a of the eigenvalues α as functions of the Marangoni number which is the relevant governing parameter for fluids of infinite Prandtl number. On the contrary to the case of a zero Prandtl number fluid, both thermal and hydrodynamic eigenvalues evolve with the Marangoni number. The behavior of the eigenvalue spectrum in the case $Pr = \infty$ is opposite to the case $Pr = 0$: the hydrodynamic eigenvalue with the lowest positive real part remains complex and its real part decreases when the Marangoni number is increased, whereas the first negative thermal eigenvalue is tending towards zero. Therefore, the end flow structure corresponds to the development of recirculation rolls near the hot wall and to the growth of a boundary layer regime close to the cold wall. This conclusion remains true until the Marangoni number reaches the critical value $Ma_c = 575$, for which the positive real part of the lowest hydrodynamic eigenvalue vanishes, the corresponding imaginary part being equal to $b = 4.8$. This means that the penetration length of the recirculation rolls becomes infinite, and that an instability in the form of transverse stationary rolls of dimensionless wave number $b = 4.8$ can spread over the whole fluid layer. However, this is not the most

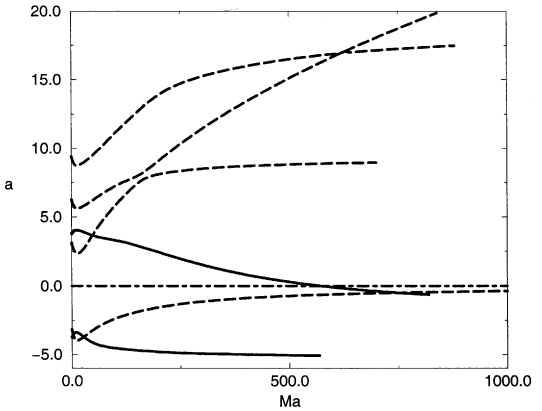

Fig. 3. Evolution of the real parts a of the eigenvalues α vs the Marangoni number Ma, in the case $Pr = \infty$. Solid lines: complex eigenvalues; dashed lines: real eigenvalues. The behavior near the hot (respectively, cold) wall is related to $a > 0$ (respectively, $a < 0$).

critical instability for an unbounded fluid layer. Indeed, Smith and Davis [6] found that a wave propagating along the direction of the imposed temperature gradient, can develop when the Marangoni number reaches the critical value $Ma_c = 399$, lower than the threshold for stationary rolls. This result valid for an infinite fluid layer, is likely to be modified by the presence of vertical end walls that prevents or delays wave propagation in the streamwise direction [26].

Villers and Platten computations [14] emphasized on the temporal behavior of the flow in finite or infinite cavity: in a closed cavity, they obtained a complex oscillatory behavior which can be decomposed in three main stages along a period. The first stage is characterized by the emission of a vortex traveling from the hot wall to the cold wall. Afterwards, the flow stabilizes in a regular multicellular pattern which is rapidly destroyed. Finally, a slowing down in the cold part of the cavity reinforces the initial hot vortex. They also considered periodic vertical boundary conditions in order to simulate the case of an infinite horizontal fluid layer and observed traveling rolls for a threshold value of the Marangoni number much lower than the threshold for oscillatory flow in a closed cavity. Despite some discrepancy in the value of the frequency they considered that their non-linear simulations confirm the linear stability results of Smith and Davis [6].

More recently, the influence of the side walls on the instability pattern has been considered by applying the concept of convective, absolute and global instability [27]. The main idea is that the global instability of spatially homogeneous systems is provided by virtual reflections of convectively unstable waves from distant lateral walls. For pure thermocapillary flows, Priede and Gerbeth [27] conclude that the threshold of the global instability is only slightly higher than that of the convective instability. For large Prandtl number, the effect of the buoyancy is to enhance the global instability threshold above the convective one.

Consideration of the two extreme cases, $Pr = 0$ and $Pr \to \infty$, has shown that the location of the recirculation rolls strongly depends on the value of the Prandtl number. In order to understand how the transition from recirculation rolls located near the cold wall for $Pr = 0$, to recirculation rolls developing near the hot wall for $Pr = \infty$ occurs, we shall consider intermediate values of the Prandtl number, varying between $Pr = 0.01$ and 100.

2.3. Intermediate values of the Prandtl number

The eigenvalues spectrum for a Prandtl number $Pr = 100$, presented in Fig. 4(a) looks very similar to the case $Pr = \infty$ presented in Fig. 3: recirculation rolls develop near the hot vertical wall whereas a boundary layer regime grows near the cold wall. A fluid of Prandtl number $Pr = 100$ is less stable with respect to stationary

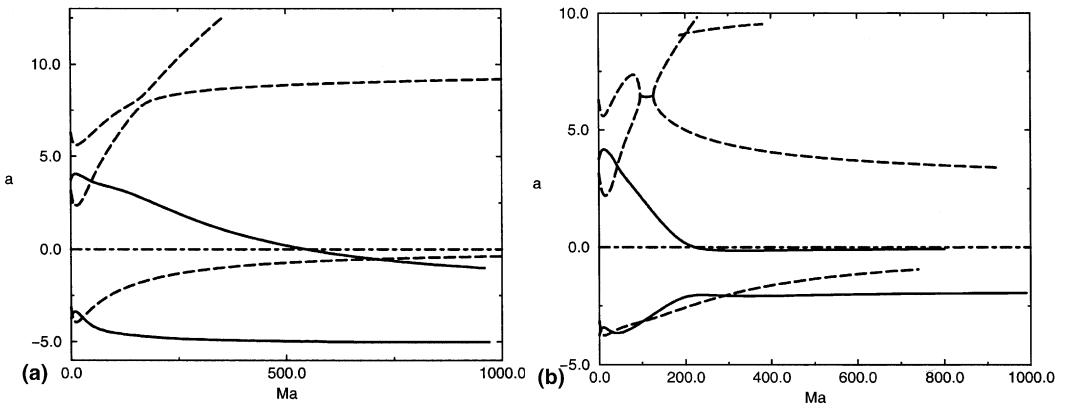

Fig. 4. Evolution of the real parts a of the eigenvalues α vs the Marangoni number Ma: (a) $Pr = 100$; (b) $Pr = 1$. Solid lines: complex eigenvalues; dashed lines: real eigenvalues. The behavior near the hot (respectively, cold) wall is related to $a > 0$ (respectively, $a < 0$).

transversal disturbances than a fluid of infinite Prandtl number, and the recirculation rolls spread over the whole fluid layer when the Marangoni number reaches the critical value $Ma_c = 547$, lower than in the case $Pr = \infty$. The wave number keeps the same value $b = 4.8$ as for $Pr = \infty$. For $Pr = 10$ and 4, the eigenvalue spectrum remains qualitatively unchanged except that the fluid becomes more and more unstable when its Prandtl number decreases: the instability threshold corresponding to the development of stationary rolls is reached for $Ma_c = 408$ with $b = 4.7$ in the case $Pr = 10$, while $Ma_c = 320$, $b = 4.3$ in the case $Pr = 4$.

For a Prandtl number equal to one, the behavior of the fluid near the cold wall becomes more intricate than for fluids of higher Prandtl numbers. The eigenvalue spectrum is represented in Fig 4(b). Recirculation rolls are still developing near the hot wall and spread all over the fluid layer when the Marangoni number reaches the value $Ma_c = 220$ associated to a wave number value $b = 2.2$, while near the cold wall a competition between a boundary layer regime and the apparition of recirculation roll takes place when the Marangoni number is increased. It is worth noticing that just before the threshold at $Ma_c = 220$, recirculation rolls exist on both sides of the cavity.

The eigenvalues spectrum for fluids of Prandtl numbers higher than one bear a close resemblance with the one obtained for an infinite Prandtl number. In particular, damped recirculation eddies are predicted to appear near the hot end wall provided that $Ma < Ma_c$. This behavior agrees with experimental observations and numerical simulations by De Saedleer et al. [3], Schwabe et al. [17], Villers and Platten [14], Favre et al. [18], Garcimartin et al. [4] and Zebib et al. [16], who observed the apparition of recirculation rolls near the hot wall.

We shall now investigate the case of fluids with Prandtl numbers smaller than one. This is first illustrated in Fig. 5(a) for a Prandtl number $Pr = 0.01$. The lower part of the spectrum corresponding to eigenvalues with negative real parts is quite similar to the same part in the case $Pr = 0$, leading to recirculation rolls developing near the cold wall, while the upper part associated to eigenvalues with positive real parts looks very different. First of all thermal eigenvalues (starting from $n\pi$ when $Re = 0$) are no more constant but evolve when the Reynolds number is increased because as soon as $Pr \neq 0$ the advection term in the heat equation triggers the coupling between the temperature and the stream function in Eq. (5). We observe that thermal eigenvalues never cross hydrodynamic eigenvalues (starting from α solution of $\sin(2\alpha) = 2\alpha$ when $Re = 0$), but follow two distinct behaviors: either repulsion or merging. In particular the thermal eigenvalue starting from π decreases suddenly when the Reynolds number reaches the value $Re = 15$ as to avoid the above real eigenvalue. This second eigenvalue belongs to the lower branch of the two real hydrodynamic eigenvalues issued from the complex hydrodynamic eigenvalue starting from $\alpha = 3.7 + i1.4$. The eigenvalue tending towards zero is still real, though it is now of the thermal type for $Pr = 0.01$, while it was of the hydrodynamic type for $Pr = 0$, and thus a boundary layer regime develops near the hot wall in both cases. Merging also occurs for eigenvalues of higher real parts: the hydrodynamic eigenvalue starting from $\alpha = 7.0 + i1.7$, splits into two real eigenvalues when $Re = 53$, and the lower branch merges with the thermal eigenvalue starting from 2π for $Re = 0$. Thus, the eigenvalue created by this process can no longer be called hydrodynamic, even though it is complex.

Although the eigenvalues spectra for the cases $Pr = 0$ and 0.01, are different the conclusions concerning the behavior of the flow near the vertical walls are the same. This is no longer true when still increasing the Prandtl number, and especially for the case $Pr = 0.1$ as illustrated in Fig. 5(b). A succession of couplings between

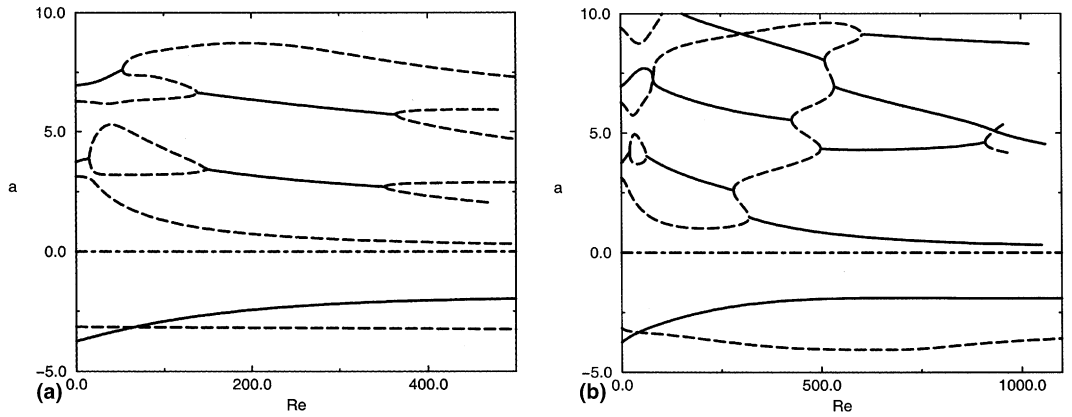

Fig. 5. Evolution of the real parts a of the eigenvalues α vs the Reynolds number Re: (a) $Pr = 0.01$; (b) $Pr = 0.1$. Solid lines: complex eigenvalues; dashed lines: real eigenvalues. The behavior near the hot (respectively, cold) wall is related to $a > 0$ (respectively, $a < 0$).

thermal and hydrodynamic eigenvalues are observed. The hydrodynamic eigenvalue starting from $\alpha = 3.7 + i1.4$ at $Re = 0$, soon experiences a first splitting followed by a quick recombination and it remains complex until the value $Re = 280$, at which it splits into a set of two real eigenvalues. Then, the lower branch of this set merges at $Re = 320$, with the thermal eigenvalue coming from $\alpha = \pi$ at $Re = 0$, giving rise to a complex eigenvalue. Therefore, the behavior of the fluid near the hot wall consists in a boundary layer regime for small values of the Reynolds number and a transition to recirculation rolls occur when $Re = 320$. Near the cold wall, ($a < 0$) the apparition of recirculation rolls is still predicted. Thus, we infer that recirculation rolls develop on both sides of the cavity for Reynolds number values higher than $Re = 320$.

We can now summarize the results: recirculation rolls develop only near the hot wall for fluid of high Prandtl numbers ($Pr \geqslant 4$), only near the cold wall for low Prandtl numbers ($0 \leqslant Pr \leqslant 0.01$), and develop on both sides for intermediate Prandtl numbers ($0.1 \leqslant Pr \leqslant 1$).

3. Conclusion

The present analysis provides a description of the end structures of a thermocapillary flow in an extended horizontal liquid layer. It involves a matching procedure between the core flow solution and a solution valid near the vertical walls. This approach is equivalent to performing the spatial stability analysis of the velocity profile valid in the core flow. The disturbances created by the vertical walls are characterized by a complex wave number and the nature of the less attenuated mode gives information on the end flow structure. According to its sign the real part, a, of the wave number (which is also the inverse of the spatial attenuation rate) describes the matching near the hot ($a > 0$) or the cold wall ($a < 0$). When it exists, the associated imaginary part reveals the existence of damped periodic structures which are known as recirculation rolls or eddies. Our analysis shows the evolution of the wave number as a function of the Reynolds or Marangoni number for different values of the Prandtl number. For large or small Prandtl numbers there is a strong asymmetry between the hot wall and the cold wall. For large Prandtl numbers the wave number attached to the hot wall is complex and signals the presence of damped recirculation eddies. This is the reverse situation which prevails for small Prandtl numbers. For intermediate values of the Prandtl number, there is always a range of Reynolds number values for which the flow is symmetrical with eddies near the hot corner and the cold corner.

Our results are in agreement with previous experimental and numerical findings and they are particularly suitable to describe the damped transverse rolls reported in [3]. Among the previous studies, several of those devoted to large Prandtl number fluids [4,14], have emphasized on the role played by the strong vortex near the hot wall for further destabilization of the flow. As soon as an oscillatory state is reached, the same scenario is reported which consists in the emission of a vortex from the hot to the cold wall. It seems unlikely that this type of oscillatory state could be explained by the onset of a global instability of the homogeneous core flow. We preferably agree with the assertion by Zebib et al. [16] that instabilities in cavities are more likely to be connected with the strong corner flow than with profiles of the type considered by Smith and Davis [6].

At this stage, more work is needed to completely understand the stability problem of the damped recirculation rolls.

References

[1] F. Daviaud, J.M. Vince, Traveling waves in a fluid layer subjected to a horizontal temperature gradient, Phys. Rev. E 48 (1993) 4432–4436.

[2] P. Gillon, G.M. Homsy, Combined thermocapillary-buoyancy convection in a cavity: an experimental study, Phys. Fluids 8 (1996) 2953–2963.

[3] C. De Saedeleer, A. Garcimartin, G. Chavepeyer, J.K. Platten, The instability of a liquid layer heated from the side when the upper surface is open to air, Phys. Fluids 8 (1996) 670–676.

[4] A. Garcimartin, N. Mukolobwiez, F. Daviaud, Origin of waves in surface-tension-driven convection, Phys. Rev. E 56 (1997) 1699–1705.

[5] M.G. Braunsfurth, G.M. Homsy, Combined thermocapillary-buoyancy convection in a cavity. Part II: an experimental study, Phys. Fluids 9 (1997) 1277–1286.

[6] M.K. Smith, S.H. Davis, Instabilities of dynamic thermocapillary liquid layers. Part 1. Convective instabilities, J. Fluid Mech. 32 (1983) 119–144.

[7] P. Laure, B. Roux, Linear and non-linear analysis of the Hadley circulation, J. Cryst. Growth 97 (1989) 226–234.

[8] G.Z. Gershuni, P. Laure, V.M. Myznikov, B. Roux, E.M. Zhukhovitsky, On the stability of plane-parallel advective flows in long horizontal layers, Microgravity Q 2 (1992) 141–151.

[9] P.M. Parmentier, V.C. Regnier, G. Lebon, Buoyant-thermocapillary instabilities in medium-Prandtl-number fluid layers subject to a horizontal temperature gradient, Int. J. Heat Mass Transfer 36 (1993) 2417–2427.

[10] J.F. Mercier, C. Normand, Buoyant-thermocapillary instabilities of differentially heated liquid layers, Phys. Fluids 8 (1996) 1433–1445.

[11] V. Sass, H.C. Kuhlmann, H.J. Rath, Investigation of three-dimensional thermocapillary convection in a cubic container by a multi-grid method, Int. J. Heat Mass Transfer 39 (1996) 603–613.

[12] H. Ben Hadid, B. Roux, Thermocapillary convection in long horizontal layers of low-Prandtl-number melts subject to a horizontal temperature gradient, J. Fluid Mech. 221 (1990) 77–103.

[13] H. Ben Hadid, B. Roux, Buoyancy- and thermocapillary-driven flows in differentially heated cavities for low-Prandtl-number fluids, J. Fluid Mech. 235 (1992) 1–36.

[14] D. Villers, J.K. Platten, Coupled buoyancy and Marangoni convection in acetone: experiments and comparison with numerical simulations, J. Fluid Mech. 234 (1992) 487–510.

[15] M. Mundrane, A. Zebib, Two- and three-dimensional buoyant thermocapillary convection, Phys. Fluids A 5 (1993) 810–818.

[16] A. Zebib, G.M. Homsy, E. Meiburg, High Marangoni number convection in a square cavity, Phys. Fluids 28 (1985) 3467–3476.

[17] D. Schwabe, U. Möller, J. Schneider, A. Scharmann, Instabilities of shallow dynamic thermocapillary liquid layers, Phys. Fluids A 4 (1992) 2368–2381.

[18] E. Favre, Convection thermocapillaire et thermogravitaire dans un fluide chauffé sur sa surface libre, Thèse de Doctorat de l'Institut national Polytechnique de Grenoble, France, 1997.

[19] E. Favre, L. Blumenfeld, F. Daviaud, Instabilities of a liquid layer locally heated on its free surface, Phys. Fluid 9 (1997) 1473–1475.

[20] P. Laure, B. Roux, H. Ben Hadid, Nonlinear study of the flow in a long rectangular cavity subjected to thermocapillary effect, Phys. Fluids A 2 (1990) 516–524.

[21] P.G. Daniels, Transition to the convective regime in a vertical slot, Int. J. Heat Mass Transfer 28 (1985) 2071–2077.

[22] J.A. Bye, Numerical solutions of the steady-state vorticity equation in rectangular basins, J. Fluid Mech. 26 (1966) 577–598.

[23] M.D. Neary, K.D. Stephanoff, Shear-layer-driven transition in a rectangular cavity, Phys. Fluids 30 (1987) 2936–2946.

[24] C. Normand, I. Mutabazi, J.E. Wesfreid, Recirculation eddies in the flow between two horizontal coaxial cylinders with a partially filled gap, Eur. J. Mech. B/Fluids 10 (1991) 335–348.

[25] J.-F. Mercier, Instabilités d'écoulements thermocapillaires et de thermogravité, Thèse de Doctorat de l'Université Paris 6, 1997.

[26] M.A. Palacho, J. Burgete, Temperature oscillations of hydrothermal waves in thermocapillary-buoyancy convection, Phys. Rev. E 59 (1999) 835–840.

[27] J. Priede, G. Gerbeth, Convective, absolute, and global instabilities of thermocapillary-buoyancy convection in extended layers, Phys. Rev. E 56 (1997) 4187–4199.